OPTICAL MODELLING: A POWERFUL TOOL IN THE ANALYSIS OF HIGHLY EFFICIENT POLYMER SOLAR CELLS

L. H. Slooff[1], S. C. Veenstra[1,5], W. Eerenstein[1,5], D. J. D. Moet[1,2], J. Sweelssen[3,5], M. M. Koetse[4,5] and J. M. Kroon[1,5]

[1]Energy research Centre of the Netherlands (ECN), PO Box 1, 1755 ZG Petten, The Netherlands, tel: +31 224 564314, fax: +31 224 56 8214, email: slooff@ecn.nl

[2]Zernike Institute for Advanced Materials, University of Groningen, Nijenborgh 4, 9747 AG Groningen, The Netherlands

[3]Science and Industry, TNO, P.O. Box 6235, Eindhoven, 5600 HE, The Netherlands

[4]Holst Centre / TNO, Hightech Campus 48, Eindhoven, 5656 AE, The Netherlands

[5]Dutch Polymer Institute, Eindhoven, NL-5600 AX, The Netherlands

ABSTRACT: We report one of the highest power conversion efficiencies (PCE) of 4.2 % (AM1.5, 1000 W/m2) for an organic polyfluorene:fullerene solar cell. Optical modeling was used to calculate whether the optical absorption and thus the short circuit current in such a solar cell can be enhanced, either in single junctions by varying the active layer thickness and applying optical spacers, or by going to a tandem structure. From a comparison of the calculated currents with measured currents, the internal quantum efficiency (IQE) was estimated, resulting in a maximum IQE of 75% for the best device. When an optical spacer is used, the thickness of the electron transport layer (ETL) and hole transport layer (HTL) is very important. The absorption in a single junction solar cell can be enhanced by 10% by reducing the HTL thickness and by inserting a thin ETL. The current density in a tandem consisting of 2 polyfluorene:fullerene blend layers is strongly dependent on the thickness of these blend layers. An increase of 20% in short circuit current is possible for a layer combination with optimized layer thicknesses and corresponding ETL and HTL layer thickness.

Keywords: polymer film, modeling, light-trapping

1 INTRODUCTION

Since the discovery of electrical conductivity in doped polyacetylene in 1977,[1] much attention has been drawn to conjugated polymers. It was realized that this class of organic materials offers advantageous properties as compared to inorganic semiconductors, like their mechanical flexibility, the tunability of their opto-electronic properties, easy incorporation in various kinds of devices and, above all, low-cost fabrication of these devices.[2] However, two main hurdles that have to be overcome are the relatively low efficiency and stability of polymer based solar cells. The efficiency of a polymer solar cell consisting of a blend of a light absorbing electron donating polymer and [C60]PCBM electron acceptor well above 2% was first reported in 2001 [3]. The highest independently verified value reported to date is 4.8% for a single junction solar cell [4] and 6% (unverified) for a tandem junction [5.

The most intensively studied combination of materials is the polymer material P3HT mixed with [C60]PCBM, for which device efficiencies between 4-5% have been reported [6,7]. P3HT:PCBM solar cells have a V_{oc} of 0.6 V, and a current density between 10-12 mA/cm^2 [4,5,8]. In recent years, polyfluorenes have gathered much attention in organic light emitting diode (OLED) research, because of their specifically good transport properties, stability (both thermal and water-/air-stability) and tunability. Polyfluorene-based polymers with lower band gap energies have been synthesized for energy conversion applications in attempts to harvest more light at higher wavelengths, i.e., beyond the visible part of the sun's spectrum. Promising results have been reported for solar cells based on various kinds of polyfluorene derivatives (see refs.[9-12] and refs. therein). Devices based on the polyfluorene PF10TBT and PCBM [13,14] have a larger V_{oc} of 1 V compared to devices of P3HT:PCBM. The optical bandgap of PF10TBT and P3HT is similar, around 2 eV, and the optical absorption of P3HT and PF10TBT are thus expected to be similar. However, the measured current density of about 8 mA/cm^2 in PF10TBT is lower. [13]. It is therefore expected that an increase in current density would lead to efficiencies above those of P3HT based devices.

In this letter, efficient, reproducible bulk heterojunction solar cells have been made by spincasting a chlorobenzene solution of poly(9,9-didecanefluorene-alt-(bis-thienylene)benzothiadiazole) (PF10TBT) as electron donor and [C60]PCBM as electron acceptor and optical modeling was used to predict the optimal light absorption and corresponding current density.

2 EXPERIMENTAL

A more detailed description on device fabrication and electrical characterization can be found in ref [15]. In short, a PEDOT:PSS (Bayer) film was spincoated on top of an indium tin oxide (ITO) covered glass substrate. Next, a polymer:fullerene solution (ratio of 1:4 by weight) was spincoated. Finally a LiF/Al counter electrode was evaporated, resulting in the following device structure Al/LiF/PF10TBT:[C60]PCBM/PEDOT:PSS/ITO/glass.

Ellipsometry measurements were carried out at the FOM institute for Atomic and Molecular Physics (Amsterdam, The Netherlands) using a Woollam VASE ellipsometer. All materials were characterised on quartz substrates except for the indium tin oxide (ITO), which was deposited on a glass substrate. Depending on the material, a Cauchy dispersion model, or a combined Lorentz, Tauc-Lorentz oscillator model was used to fit the measured ellipsometry parameters Ψ and Δ.[16]

The lamp spectrum was measured using an AVANTES AVASPEC 2048 fibre optic spectrometer. To collect radiation over 180^o a CC-UV/VIS cosine corrector is attached to the optic fibre. Before measuring the lamp spectrum an intensity calibration is done using an AVANTES HL-2000-CAL tungsten halogen calibration lamp.

Power conversion efficiencies (PCE) were measured under 1000 W/m^2, simulated AM1.5 illumination from a WXS-300S-50 solar simulator (WACOM ELECTRIC Co.). The mismatch factor (0.99) was calculated using a recent spectrum of the simulator lamp and the tabulated AM1.5 GN spectrum, the spectral responses of respectively the used filtered Si reference cell (calibrated at Fraunhofer ISE, Freiburg) and the polymer:fullerene cell.

3 RESULTS AND DISCUSSION

3.1 Single junction devices

Figure 1 shows the current-voltage measurement of the best PF10TBT:[C60]PCBM device (PF10TBT M_w = 34.9 kg/mol; poly dispersity index (PDI) = 3.6) together with the material structure. The open-circuit voltage (V_{oc}) amounted to 999 mV, the short circuit current (J_{sc}) to 7.7 mA/cm^2 and the fill factor (FF) to 54 %, resulting in a PCE of 4.2 % (estimated error 5% rel.) for a cell area of 0.36 cm^2 and a layer thickness of 186 nm. This PCE is among the highest reported for polyfluorene:fullerene photovoltaic cells and approaching the verified polymer:fullerene world record efficiency of 4.8%.[4]

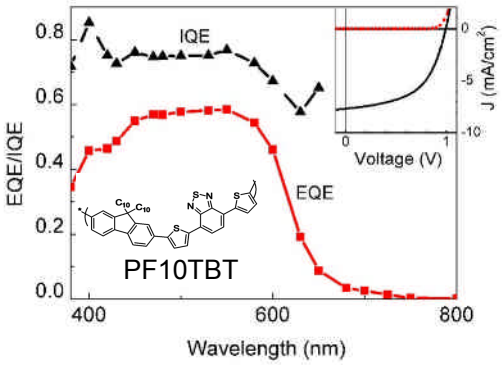

Figure 1: External quantum efficiency (EQE) measurements of the best PF10TBT: [C60]PCBM photovoltaic cell at short circuit conditions and calculated internal quantum efficiency (IQE). The inset shows the current-voltage measurement of the same device in the dark (squares) and under 1000 W/m^2 simulated AM1.5 illumination (solid line). Also shown is the molecular structure of PF10TBT.

Our latest results are slightly higher then the 3.9 % (cell area 0.36 cm^2) reported previously [15] for similar devices, where we used a PF10TBT batch with a higher molecular weight (M_w = 58.4 kg/mol; PDI =3.3). The batch with the high molecular weight was used in the remainder of this letter.

The external quantum efficiency (EQE), measured at short circuit current conditions, of the best device is shown in Fig. 1. As can be seen, in the peak at 550 nm, almost 60% of the incident photons lead to a current in the external circuit. The calculated current based on the overlap between the EQE spectrum and the AM1.5 spectrum is 7.8 mA/cm^2 which nicely corresponds with the measured AM1.5 current of 7.7 mA/cm^2. From EQE measurements it cannot be concluded whether the remaining 40% of photons is not absorbed, or are absorbed but not contributing to collected charges at the electrodes. In order to distinguish between the two options, optical modelling of these devices must be performed. There are a few reports on the optical modelling of polymer solar cells, showing that optical modelling is a powerful tool in addressing the efficiency of light absorption in the active layer.[17-19]

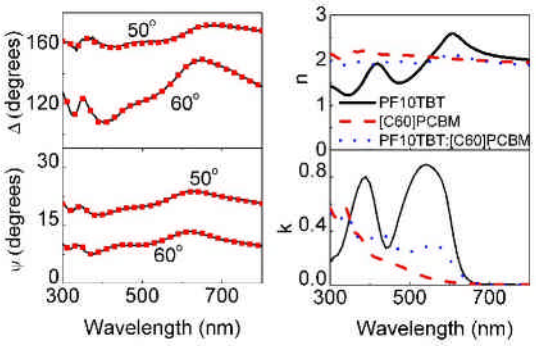

Figure 2: a) Ellipsometry parameters Ψ and Δ as a function of wavelength for a 200 nm thick film of PF10TBT:[C60]PCBM on quartz; Experimental data (solid line) and the fit of the dispersion model (squares). b) Refractive index n (top) and extinction coefficient k (bottom) as derived from ellipsometry measurements for PF10TBT (solid line), C60-PCBM (dashed line), and a 1:4 blend of PF10TBT:[C60]PCBM (dotted line).

Before calculating the light absorption distribution in the cell, ellipsometry measurements were performed to determine the optical constants of the different layers in the cell. The model fit to the experimental data for the PF10TBT:C60-PCBM blend material is shown in Fig. 2a. As can be seen the fit shows excellent agreement with the measured data. There are reports in literature on similar materials, showing that the pure polymer material has anisotropic optical constants.[19,20] However, we did not find any indication for anisotropy in the PF10TBT film. From the model fit, the wavelength dependent refractive index n and extinction coefficient k can be derived and the result is shown in Fig. 2b for the 1:4 PF10TBT:[C60]PCBM film as well as for the pure PF10TBT and [C60]PCBM materials. The maximum k of the pure PF10TBT is comparable with the k value obtained for transmission measurements, for which the film thickness was determined using a Dektak surface profiler. This k value is rather high compared to that reported for a similar polymer material.[20] The difference might be due to different stacking in the polymer film resulting from the difference in branching of the polymer side groups. The optical constants of the glass substrate, ITO, PEDOT:PSS, LiF and Al films were also derived using ellipsometry.

The optical constants were subsequently used to calculate the absorption distribution in the optical software program SCOUT21 which uses a transfer matrix formalism.[22] The absorption distribution, $dA(\lambda)/dz$, is shown in Fig. 3 for different wavelengths of the incident photons. The interference patterns resulting from the multiple reflections at the various interfaces are clearly

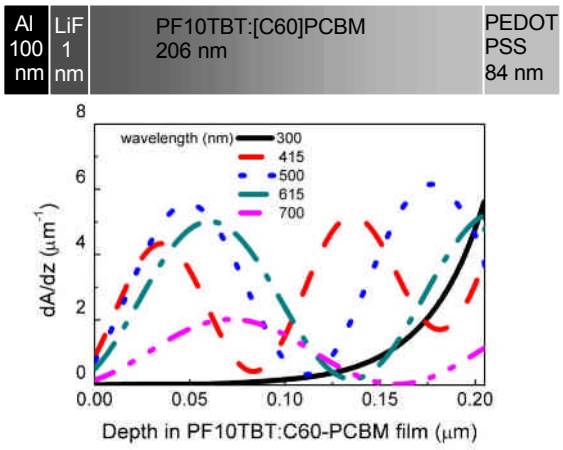

Figure 3: Absorption distribution within the active layer of a PF10TBT:[C60]PCBM photovoltaic solar cell for various wavelength of the incident light.

seen. The positions of the interference peaks shift as the wavelength of the incident photons changes. The absorption distribution was used to calculate the internal quantum efficiency (IQE) spectrum for the best device. This was done by integrating the calculated d*A*/d*z* spectrum for different wavelengths, as calculated for this device, over the film thickness. This gives the absorption spectrum in the active layer. Next, the EQE spectrum as shown in Fig. 1 is divided by this calculated absorption spectrum to give the IQE spectrum. The result is shown in Fig. 1. As can be seen, the average IQE is around 75%.

The absorption distributions were also used to calculate the total number of absorbed photons in the film. A wavelength range of 300-800 nm was selected for the incident photons as it coincides with the absorption bands of the PF10TBT and [C60]PCBM. For all these wavelengths the absorption distribution was calculated

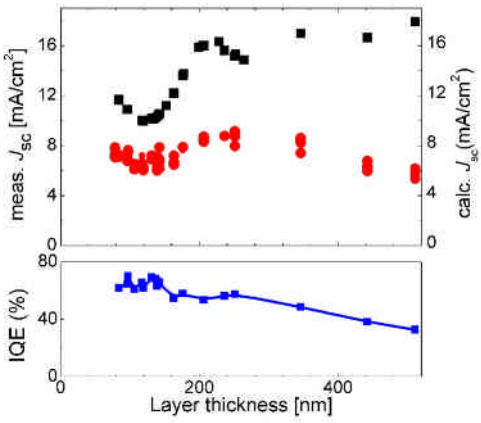

Figure 4: Top: Measured (circles) and calculated (squares) short circuit current as a function of PF10TBT:[C60]PCBM film thickness. For the calculations, the film thickness of the PEDOT:PSS and blend films of the actual devices was used. Bottom: Total internal quantum efficiency ($J_{measured}/J_{calculated}$) as a function of layer thickness.

and integrated over the film thickness to obtain the absorption spectrum $A(\lambda)$ of the film. By taking the convolution of this absorption spectrum with the number of photons in the lamp spectrum ($N_{lamp}(\lambda)$), the total number of absorbed photons per wavelength was calculated. A final integration over the wavelength range then results in the total number of absorbed photons N.

$$N = \int A(\lambda) \times N_{lamp}(\lambda) d\lambda$$

Assuming that every absorbed photon results in the collection of charge carriers in the external circuit of the device, i.e. an internal quantum efficiency (IQE) of 100%, the upper limit for the short circuit current density ($J_{sc,\,max}$) can be calculated. The result is shown in the top part of Fig. 4 as function of the layer thickness. Also shown is the measured short circuit current density (J_{sc}) for a number of PF10TBT:[C60]PCBM photovoltaic cells of various thickness. As can be seen, for thin films up to a thickness of 150 nm, the calculated current shows the same trend as the measured current, but with a certain offset. For thicker films, the measured current becomes much lower than the calculated current. This implies that the IQE is decreasing for increasing film thickness. This change in IQE with film thickness is shown in the lower part of Fig. 4 in which the ratio between the measured J_{sc} and calculated $J_{sc,\,max}$ is plotted. This ratio can be understood as the total IQE, i.e. the IQE averaged over the whole absorption spectrum. From this graph it can be concluded that up to a thickness of roughly 140 nm, 66% of the absorbed photons result in collected charge carriers at the electrodes. This is slightly lower than the IQE calculated for the device in Fig. 1. This shows that the better performance of the device in Fig. 1 is at least partly due to better charge collection. For film thicknesses above 140 nm, charge collection starts to become limiting, reducing the IQE substantially. The trade off between light absorption and collection efficiency limits the current density, and thus the performance of PF10TBT:[C60]PCBM solar cells. It is thus interesting to investigate whether it is possible to increase the light absorption in a blend layer by using optical spacer layers.

We calculated whether the optical absorption, and corresponding current density, in PFTBT:[C60]PCBM single junction solar cells can be increased by adding an optical spacer. ZnO was chosen as optical spacer material (and also functions as ETL), because flat layers can be prepared by spincoating from a solution of ZnO nanoparticles, making an anneal step unnecessary [23,24]. In Fig. 5a we show that the calculated absorption in a PFTBT:[C60]PCBM blend layer (on glass, 150 nm ITO and 80 nm PEDOT:PSS, with a LiF/Al top electrode) can increase or decrease, depending on the thickness of both the ZnO and the blend layer. For a 150 and 180 nm thick blend layer, the absorption is maximum when the ZnO spacer layer is 30 nm thick. Also shown is the experimentally determined J_{sc} for a 120 and 180 nm blend layer, without a ZnO layer and with a 30 nm ZnO layer. As can be seen, the measurement corresponds with the calculated absorption, except from a small offset. For the 150 nm and 180 nm blend layers, the absorption is also calculated as a function of the PEDOT layer thickness, both with and without a 30 nm ZnO layer, as

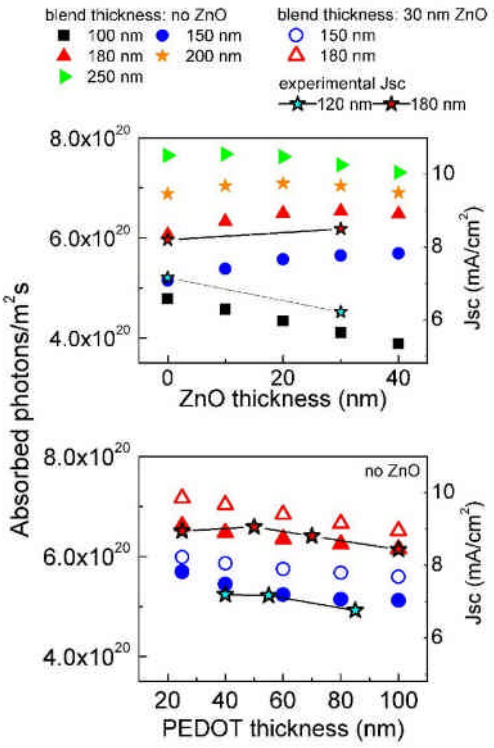

Figure 5: (top) calculated optical absorption and measured J_{sc} in a PFTBT:[C60]PCBM blend layer as a function of the thickness of the ZnO optical spacer, for blend thicknesses 100-250 nm. (bottom) calculated absorption and measured J_{sc} as a function of the PEDOT layer thickness for two blend thicknesses, with and without a 30 nm ZnO layer.

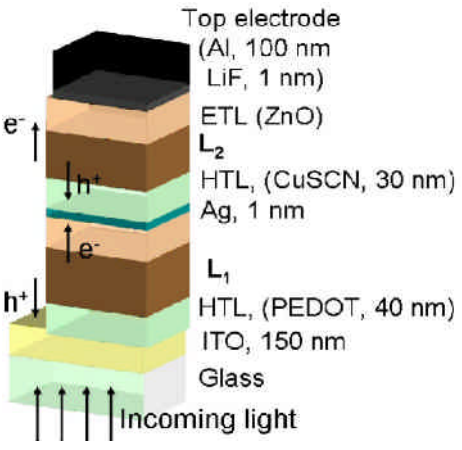

Figure 6: Structure of the tandem cell in a series configuration. On the glass substrate, a 150 nm ITO and a hole transport layer (e.g. PEDOT:PSS) serve as hole collecting bottom contact. The polymer blend layers L_1 and L_2 consist of PF10TBT:[C60]PCBM. The two blend layers are separated by ZnO (electron transport) and CuSCN (hole transport), where a very thin Ag layer serves as a recombination layer. The top electron collecting contact consists of 1 nm LiF and 100 nm Al.

shown in Fig. 5b. The measured AM1.5 current density in a 120 nm and 180 nm PFTBT device without ZnO and was also measured and shown in Fig. 5b. The trend in the measured Jsc corresponds nicely with the trend in the calculated absorption. The gain in current density by reducing the PEDOT layer and inserting a 30 nm ZnO layer is calculated from the absorption in Fig. 5b to be about 1 mA/cm^2, an increase of just over 10%.

3.2 Tandem devices

The tandem structure is shown in Fig. 6, where the ETL on the first subcell is ZnO (30 nm). Since ZnO can also act as an optical spacer, we will also consider the influence of this layer on top of the second subcell. The HTL on the ITO/glass is PEDOT:PSS. Both PEDOT:PSS and CuSCN are identified as candidates for the HTL below the second subcell. PEDOT:PSS is an acidic solution and will damage ZnO. CuSCN dissolved in dipropyl sulfide has been used as hole transporting material in dye solar cells [25] and might be more suitable. To study the influence of both polymer blend layer thicknesses, the thickness of the PEDOT:PSS, ZnO and CuSCN layer have all been fixed, as indicated in Fig. 6. The blend layer thicknesses modeled range from 50-275 nm. The Al top electrode optically acts as a mirror, resulting in interference effects in the blend layers. Therefore, the absorption in both layers is influenced by a change in either of the thicknesses.

The maximum current in the tandem cell is determined by the polymer blend layer with the lowest current density. The maximum current density in the tandem cell has been calculated using the IQE values of 0.75, 0.6 and 0.5 for film thicknesses ≤ 150 nm, 150-275

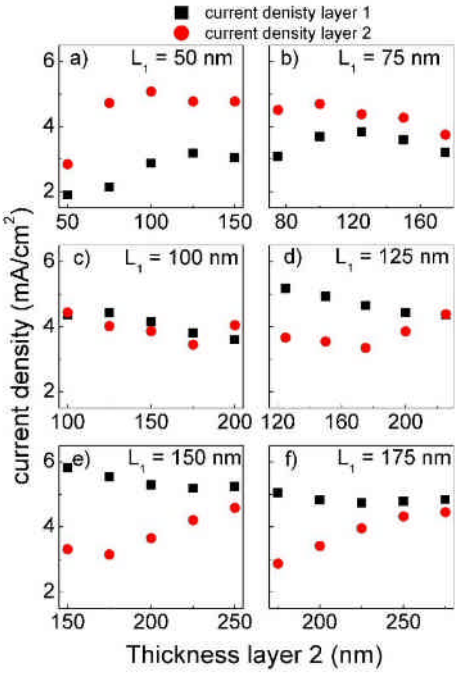

Figure 7: Calculated current densities in both layer 1 (black squares) and layer 2 (red circles) in a tandem structure. The thickness of layer 1 is a) 50 nm, b) 75 nm, c) 100 nm, d) 125 nm, e) 150 nm and f) 175 nm.

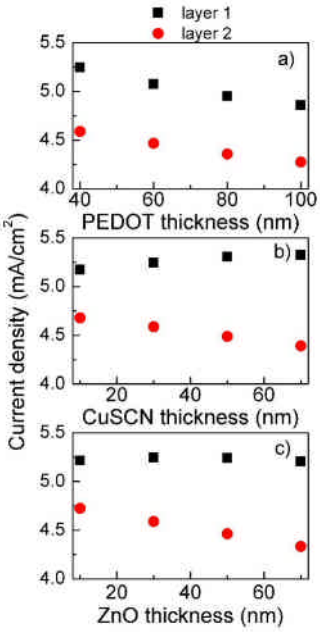

Figure 8: Current density in L1 (150 nm, black squares) and L2 (250 nm, red circles) as a function of the thickness of a) PEDOT layer thickness, b) CuSCN layer thickness and c) ZnO layer thickness determined assuming IQE = 0.75 for L1 and 0.6 for L2.

nm and 275-375 nm respectively. The limiting current density is shown in Fig. 7. Due to interference effects, the optical absorption, and thus the current, in layer 1 is lower than in layer 2 when the thickness of layer 1 is only 50 or 75 nm, thus layer 1 is then current limiting. When L1 is 100 nm, L2 has to be 200 nm thick in order to be current limiting. When L1 is 150 nm or thicker, L2 is always current limiting.

In Fig. 7, it can be seen that the largest current density of 4.6 mA/cm^2 is obtained when L1 is 150 nm and L2 is 250 nm thick. For a single solar cell of this material, the largest measured AM1.5 current density is around 8 mA/cm^2 for a film about 180 nm thick [13]. The maximum Voc that can be expected for this tandem cell is 2 V, assuming each subcell produces a Voc of 1 V like in the single solar cell. Assuming no other losses, the efficiency of this tandem structure can be 15% more than for a single cell. Fig. 7 also shows the importance of the right thickness combinations, as the values for the limiting current density differ by more than a factor 2. Optical modeling is thus a very helpful tool in choosing appropriate device configurations.

The amount of light that is absorbed in the blend layers also depends on the thickness of the other layers in the tandem structure, such as CuSCN, PEDOT and ZnO. For the tandem structure with L1 = 150 nm, and L2 = 250 nm, we calculated the absorption in both blend layers for a CuSCN and ZnO (on L1) layer thickness of 10, 30, 50 and 70 nm, and for a PEDOT layer thickness of 40, 60, 80 and 100 nm, as shown in Fig. 8. When the thickness of one of these layers is varied, all other layer thicknesses are kept constant at the same values as in Fig. 6. From Fig. 8 it can be seen that the largest current density in L2 is obtained for a ZnO and CuSCN layer of 10 nm thickness, and a PEDOT layer of 40 nm thickness. In principle, the current would be even higher for a PEDOT

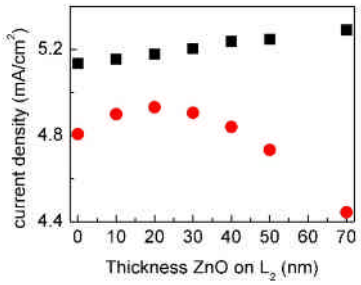

Figure 9: Influence of a ZnO spacer layer on top of the second subcell on the current density in layer 1 (150 nm) and in layer 2 (250 nm).

film thickness < 40nm, but such a thin film would result in shorts in the device. If we take all these values into the tandem structure, the maximum current density is 4.8 mA/cm^2, resulting in a maximum efficiency increase of 20% compared to a single cell device.

The optical absorption and current density in L2 could further be enhanced by putting a ZnO layer on top of L2. This is calculated for the same tandem structure, with L1 = 150 nm, and L2 = 250 nm, ZnO and CuSCN are both 10 nm and PEDOT is 40 nm like above, and shown in Fig. 9. The absorption in L2 is only increased for ZnO layer thicknesses of 10 and 20 nm. The corresponding current density, assuming the IQE = 0.6, is 4.9 mA/cm2.

With a maximum limiting current density of 4.9 mA/cm2 the overall performance of the tandem cell could ideally be 23% larger than for the measured single cell device [13]. This is assuming that each subcell produces the same voltage as a single cell device, and there are no further losses in fill factor. It was shown that along with the reduction in IQE with film thickness, the fill factor reduces as well [15]. Besides electron and hole transport, the function of the ZnO and CuSCN layers is also to protect the bottom polymer blend layer from being damaged, it is necessary that these layers are closed and flat. It is not known if very thin films of only 10 nm will be closed, and thus experimentally this thickness might be too thin. Taking all these factors into account, it is not likely that the total efficiency of an optimized tandem cell, with identical materials in the two subcells, will exceed the efficiency of an optimized single junction solar cell, despite the fact that in a single cell with maximum current density not all light is absorbed. Therefore we conclude that, apart from the increased complexity of processing tandem structures, it will be more fruitful to optimize a single cell device by reducing the PEDOT:PSS layer thickness and by inserting a thin ZnO layer. For improved tandem performance, two materials with different bandgaps are needed, such as PF10TBT and the recently published low band gap material PCPDTBT [26]. Also, when materials with different bandgaps are employed, the right thickness combination will be important for obtaining optimal current densities, and the modeling process described here will be necessary.

4 CONCLUSIONS

The optical absorption in solar cells consisting of a

single junction of PF10TBT:[C60]PCBM can be enhanced 10% by inserting a thin (30 nm) electron transport layer (ZnO) which also acts as an optical spacer, and by reducing the thickness of the hole transport layer (PEDOT). The current density in a tandem structure consisting of two PF10TBT:PCBM blend layers is strongly dependent on the thicknesses of both blend layers, and achieves a maximum for a combination of film thicknesses of 150 nm and 250 nm. This thickness combination, combined with a thin HTL and two ETL layers could lead to an increase around 20%, assuming no losses in V_{oc} and fill factor. As those losses are likely to occur, the total performance of a tandem cell is not likely to be more than for a single junction solar cell of PFTBT:[C60]PCBM, and it will be more fruitful to optimize a single junction device. Tandem cells will only become an interesting alternative if low bandgap polymers become available.

6 ACKNOWLEDGEMENTS

This work was funded by SenterNovem via the EOS Long Term program ZOMER (EOS LT 03026).
FOM-Amolf is greatly acknowledged for the opportunity of performing ellipsometry measurements.

[1] C. K. Chiang, C. R. Fincher Jr., Y. W. Park, A. J. Heeger, H. Shirikawa, E. J. Louis, S. C. Gau, and A. G. MacDiarmid, Phys. Rev. Lett. **39** (1977) 1098
[2] J. -M. Nunzi, C. R. Physique **3** (2002) 523
[3] S.E. Shaheen *et al*, Appl. Phys. Lett **78** (2001) 841
[4] M. A. Green, K. Emery, D. L. King, Y. Hishikawa and W. Warta, Prog. Photovolt: Res. Appl. **14** (2006) 455
[5] J. Y. Kim, K. Lee, N. E. Coates, D. Moses, T-Q. Nguyen, M. Dante, A. J. Heeger, Science **317** (2007) 222
[6] C. Waldauf C. Waldauf, M. Morana, P. Denk, P. Schilinsky, K. Coakley, S. A. Choulis, and C. J. Brabec, Appl. Phys. Lett. **89** (2006) 33517
[7] W. Ma, C. Yang, X. Gong, K. Lee, A. J. Heeger, Adv. Funct. Mat. **15**, 1617 (2005).
[8] V. Shrotriya, G. Li, Y. Yao, T. Moriarty, K. Emery, Y. Yang, Adv. Funct. Mat. **16** (2006) 2016
[9] M. Svensson, F. Zhang, S. C. Veenstra, W. J. H. Verhees, J. C. Hummelen, J. M. Kroon, O. Inganäs, and M. R. Andersson, Adv. Mater. **15** (2003) 988
[10] F. Zhang, K. G. Jespersen, C. Björström, M. Svensson, M. R. Andersson, V. Sundström, K. Magnusson, E. Moons, A. Yartsev, and O. Inganäs, Adv. Funct. Mater. **16** (2006) 667
[11] R. Pacios, D. D. C. Bradley, J. Nelson, and C. J. Brabec, Synth. Met. **137** (2003) 1469
[12] Q. Zhou, Q. Hou, L. Zheng, X. Deng, G. Yu, and Y. Cao, Appl. Phys. Lett. **84**, 1653 (2004).
[13] L. H. Slooff, S. C. Veenstra, J. M. Kroon, D. J. D. Moet, J. Sweelssen, M. M. Koetse, Appl. Phys. Lett. **90** (2007) 143506
[14] A. Gadisa *et al*, Thin Solid Films **515** (2007) 3126
[15] D. J. D. Moet L. H. Slooff, J. M. Kroon, S. S. Chevtchenko, J. Loos, M. M. Koetse, J. Sweelssen, and S. C. Veenstra, Mat. Res. Soc. Symp. Proc. **974** (2007) 0974-CC03-09
[16] J. A. Woollam, B. Johs, C. M. Herzinger, J. Hilfiker, R. Synowicki, and C. L. Bungay, Critical Rev. Opt. Science Techn. **CR72** (1999) 3
[17] H. Hoppe, N. Arnold, N. S. Sariciftci, D. Meissner, Sol. Energy Mater Sol. Cells **80** (2003) 105
[18] H. Hoppe, N. Arnold, D. Meissner, N. S. Sariciftci, Thin Sol. Films **451-452** (2004) 589
[19] N-K. Persson, H. Arwin, O. Inganas, J. Appl. Phys. **97** (2005) 034503
[20] N-K. Persson, M. Schubert, O. Inganäs, Sol. Energy Mater Sol. Cells **83** (2004) 169
[21] W.Theiss Hard- and Software, Dr.-Bernhard-Klein-Str. 110, D-52078 Aachen, Germany; www.mtheiss.com.
[22] O. S. Heavens, *Optical properties of thin films*, (Dover Publications, New York, 1991).
[23] J. Gilot, M. M. Wienk, and R. A. J. Janssen, Appl. Phys. Lett. **90** (2007) 143512
[24] W. J. E Beek, thesis University of Eindhoven, The Netherlands (2005)
[25] B.C. O'Regan and F. Lenzmann, J. Phys. Chem B **108** (2004) 4342
[26] D. Mühlbacher, M. Scharber, M. Morana, Z. Zhu, D. Waller, R. Gaudiana, C. Brabec, Adv. Mat. **18** (2006) 2884